User Terminal Planar Antennas for Wireless Broadband Access at K_a Satellite Band

Filipe Faria
filipe.faria@tecnico.ulisboa.pt
Universidade de Lisboa
Instituto Superior Técnico, Lisboa, Portugal

January 2021

Abstract

Millimetre waves satellite communications systems are emerging as a viable solution to provide global broadband coverage. This endeavour poses several new challenges for the antenna design. Radial Line Slot Array (RLSA) antenna is a conventional leaky wave antenna that can be adapted to the new specifications of ground or space terminals, featuring high gain, low profile, and low cost. This work presents a comprehensive study on the design of RLSA's, which requires an arrangement of a spiral like distribution of sub-wavelength slots in the upper plate of the circular parallel plate waveguide that compose the antenna. There is a wide variety of trade-offs to be considered in terms of the radiation and aperture efficiencies, bandwidth, cross-polarization, side lobe level and return losses. To have a systematic design method, two tools were developed: i) a GO/PO (Geometric Optics/ Physical Optics) framework for defining the antenna geometry; ii) a macro procedure that constructs the CAD (Computer Aided Design) model of the antenna for the full-wave analysis. Two antenna designs are presented in this work operating at 29.1 GHz: a RLSA that produces a boresight collimated beam with a 29.3 dBi gain; a second design that generates a 25.4^{o} offset collimated beam with 26.4 dBi gain. Both designs have a diameter of 150 mm with only 1.61mm of height. A cavity-based feeding structure was also developed and optimized in order to simplify the manufacturing complexity of the RLSA antennas. Prototypes are being fabricated and measured, aiming to experimentally validate the promising full-wave results.

Keywords: satellite communications, leaky-wave antennas, CP-RLSA, beam-tilt, feeding cavity

1. Introduction

In recent years, there has been an increase in the way information is accessed across the globe. There is a need for a reliable system which provides a high coverage area and a fast and strong connection. In response to this challenge, SOTM (Satcom On the Move) broadband access services with LEO (Low Earth Orbit) and MEO (Medium Earth Orbit) are being developed. This growing trend in the of satellite-based services require an alternative equivalent solution: a small, thin, light, and low-cost structure. This way a more widely available option can be produced. RLSA (Radial Line Slot Array) antennas are studied. A RLSA antenna is circular structure comprised of two parallel plates and fed in the centre, normally by a coaxial cable. Top plate is covered with slots to allow radiation to escape. The slot positioning, dimensions and angle orientation and antenna diameter and thickness are key features of the design. K. Kelly and F. Goebels, in 1963, present the first developments of RLSA antenna. The antenna prototypes work with crossed slots and can operate using circular, linear, or elliptical polarization depending on the feed circuit [2]. In 1986, Ando et al. presented a design for a double-layered CP-RLSA (circular polarized RLSA). A practical theoretical foundation for the antenna design and equations are presented to place the slot pairs [6][5]. In 1990, Ando et al, propose a new SL-RLSA (single layered RLSA) with circular polarization. A single layered RLSA requires a simpler fabrication process and a costs reduction overall. Two new techniques to improve antenna efficiency are also introduced: slot length and spacing variation and a matching spiral [7][4]. In 1995, Takashi et al., introduce and apply beam tilting to a CP-RLSA by distributing the slot pairs over an elongated spiral. A 50 cm diameter antenna is design with good efficiency and gain values [9]. In 2003, M. Vera-Isasa et al., publish a new design method for a beam tilted CP-RLSA. A good cross polarization ratio and directivity are achieved for an antenna working at 12.1GHz with a 10^{o} tilt angle [10]. In 2012, M. Albani et al., present a computational procedure to reduce higher spurious of electromagnetic (EM) wave modes from propagating and to perform beam shaping. Three models for CP-RLSA are designed based: pencil beam shape with controlled side lobe level (SLL), Isolux pattern, and pencil beam shape for maximum directivity pattern. All work at 22 GHz and present good total efficiency and good gain performance [3].

In 2015, T. Nguyen et al., minimize the dielectric losses and enhance the antenna gain trough a new formulation for aperture slot coupling control in a 40 cm diameter CP-RLSA working at 60GHz [11]. More recently, in 2020, new approaches continue to exist in the design of RLSA's. M. Lopez-Morales et al. present a combination of both a new analytic approach with optimization techniques based on current distribution, and energy conservation inside the antenna. The proposed design has gain of 35.6dBi ate 20GHz [8].

2. Formulation and Methods

RLSA antennas are a form of leaky-waveguide antenna. They consist of a circular parallel plate waveguide (PPW) which is fed an outward travelling wave. The wave is then radiated by cutting slots into the top plate of the antenna. Slot dimensions and orientation will determine the type of wave synthesized. A rudimentary example of how it works is shown in Figure 1. The structure is dependent on key elements which affect antenna performance and beam synthesis.

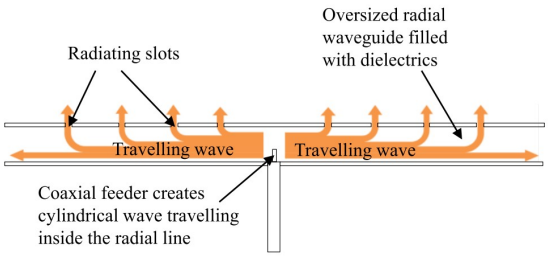

Figure 1: Example of how a RLSA works [11]

2.1. PPW – Parallel Plate Waveguide

The waveguide is comprised of two circular parallel plates. An important feature to consider when designing the plates is the diameter. The larger the diameter, the longer a wave is propagated towards the edges. Thus, more power escapes trough the slots and less residual power remains inside the PPW. Oppositely, the diameter cannot be too small because the waveguide would retain a large part of the power and interference issues would emerge. This residual power is expected to cause return loss problems. The height between the two plates is also a key aspect to take into consideration. To allow only the fundamental cylindrical mode $TM^{z}_{0,0}$ to propagate inside the waveguide the distance must obey the following condition [6]:

$$d < \frac{\lambda_g}{2} \tag{1}$$

Where, d represents the distance between the places and λ_g represents the guided wavelength. The guided wavelength is given the equation [1]:

$$\lambda_g = \frac{\lambda_0}{\sqrt{\epsilon_r}} \tag{2}$$

2.2. Slot Pair for Circular Polarization

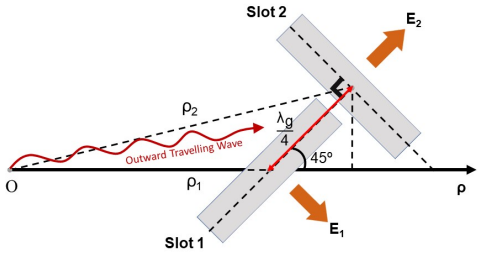

Figure 2: Slot Pair RHCP key features to generate orthogonal fields with a time-phase difference of $\frac{\pi}{2}$ radians

The slots are arranged in a particular manner to achieve circular polarization. This involves the electric or magnetic field vector trace a circle in space as a function of time and there are three conditions to accomplish such polarization. First, the field is required to have two orthogonal linear components, meaning, the field components have a 90^o difference in space. Second, those two components must have the same magnitude. And finally, the field components must have a time-phase difference of odd multiples of $\frac{\pi}{2}$ radians, which is equivalent to delaying one of the components by referred sum. These three conditions are necessary and sufficient to realize circular polarization [1]. A slot pair must be designed to implement these conditions. Each unit of the array contains a pair of slots that are placed orthogonally. This translates to a 90^o angle between the two slots and 45^o angle between the first slot and the radial direction. The orthogonal placement is responsible for generating two orthogonal electric field. If the slots are placed as shown in Figure 3, RHCP (Right hand circular polarization) is achieved. If they each individual slot in Figure 3 is rotated by 90^o then, LHCP (Left hand circular polarization) is achieve. Next, to produce the same field magnitude, the slots are equal in size. Both length and width are kept the same in a slot pair. Lastly, to secure a phase difference of $\frac{\pi}{2}$ radians between both generated fields, the following condition is applied based on Hankel functions[6]:

$$\arg(\, H_1^{(1)}(k_g \rho_2)\,) \;-\; \arg(\, H_1^{(1)}(k_g \rho_1)\,) \;=\; \frac{\pi}{2} \tag{3}$$

By simplifying the previous criteria, the two slots are separated by a quarter of λ_g. Thus, to establish the distance between slots the following expression is used as in reference [6]:

$$\rho_2 - \rho_1 = \frac{\lambda_g}{4} \tag{4}$$

2.3. Aperture distribution

The fields inside the PPW are given by an asymptotic approximation of the Hankel Functions. When $k_g\rho >> 1$, the following describes the magnetic field inside [6]:

$$H_\varphi = H_1^{(1)}(k_g\rho) \approx \sqrt{\frac{2}{\pi\, k_g\rho}} e^{-j(k_g\rho - \frac{3\pi}{4})} \quad (5)$$

where ρ is the radial coordinate, and k_g is the guided wave number. The slots are placed in helicoidal distribution to maximize the number of slots over the aperture. All the contributions of the individual slot pairs accomplish a directive beam. However, when making the spiral arrangement, slot pairs need to keep their relative angle with respect to radial direction for all the rotations. This means every azimuthal rotation is responsible for adding a phase factor $e^{-j\phi}$ the slot placement must compensate so that all the radiating slots are fed in phase [6]. Slot pair density over top plate is defined as: Sϕ x Sρ. Sϕ is the azimuthal distance between adjacent slot pairs and Sρ is the radial spacing between slot pairs [3]. Sϕ is defined arbitrarily, and various values are considered throughout the work. The phase factor compensation mentioned before is responsible for making Sρ value defined as a guided wavelength, λ_g. From [6], to obtain the angle of rotation for each slot pair for an arbitrary arc length, a line integral equation is derived:

$$\rho d\theta = \rho_0 d\theta + \theta\frac{\lambda_g}{2\pi}d\theta = dl \quad (6)$$

The arc length is symbolized by dl. Let us call it arclen from now onwards. Next, the equation is solved:

$$arclen = \int_{\theta_1}^{\theta_2} \rho_0 d\theta + \frac{\lambda_g}{2\pi}\int_{\theta_1}^{\theta_2} \theta\, d\theta \quad (7)$$

$$\theta_2{}^2 + 2k_g\rho_0\theta_2 - (2k_g arclen + 2k_g\rho_0\theta_1 + \theta_1^2) = 0 \quad (8)$$

Now we solve for θ_2 using a simple quadratic formula and get:

$$\theta_2(\theta_1) = -k_g\rho_0 + \sqrt{(k_g\rho_0)^2 + 2k_g arclen + 2k_g\rho_0\theta_1 + \theta_1{}^2} \quad (9)$$

The newly defined arclen represents the same as the azimuthal distance between two radiating slot pairs, Sϕ.

2.4. Feeding Structure

The approach regarding a feeding structure is initially as described for single-layered RLSA. The construction complexity and height of a DL-RLSA, makes it undesirable to pursue such configuration. It is well established in literature the obvious evolution and allure of opting for a SL-RLSA. Complexity in no longer an issue but instead precision is. The substrate layer can reach small and thin dimensions in size and it becomes difficult to tweak the cable position inside the waveguide. Due to such manufacturing constraints concerning the precision of the cable, a hybrid version is proposed to establish an accessible and simple construction process. This hybrid feed consists of opening a circular hole on the bottom plate and then connecting it to small opened-ended cavity. Naturally, the proposed cavity is cylindrical and placed in line with the antennas' centre to produce an outward travelling wave.

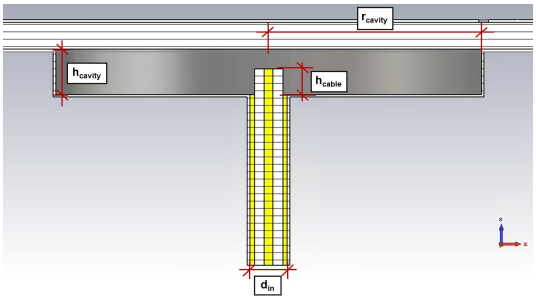

Figure 3: RLSA Feeding solution proposed. The dimensions are represented by the following variables: h_{cavity} – height of the cavity, h_{cable} – height of then cable inside the feed, din – diameter of the opening for cable insertion and r_{cavity} – the radius of the cylindrical cavity.

To achieve a good coupling between the feed and the upper waveguide, a similar approach to the PPW height is considered. To avoid higher modes from propagating inside the feed, the height follows the condition described in equation (1). Thus, making sure the feeding wave only propagates in the fundamental mode $TM^z_{0,0}$.

2.5. Beam-Tilt Design

By producing a regular slot spiral, the boresight direction is at 0^o and by producing a spiral with an elongated shape, the beam direction tilts accordingly. To place the slots in the right position, the following equations must be met [9]:

$$\rho_s(\varphi) = \frac{\varphi}{k_g - k_0 \sin\alpha_0 \cos\varphi} \quad (10)$$

Where ρ represents the radial distance, k_0 and k_g are the wavenumbers in free-space and guided inside the PPW, respectively. α_0 is the angle chosen for the beam tilt and φ represents the azimuth of the slot pairs. From equation (2) and from k_0 and k_g:

$$\rho_s(\varphi) = \frac{\frac{1}{k_0\sqrt{\epsilon_r}}\varphi}{1 - \frac{\sin\alpha_0}{\sqrt{\epsilon_r}}\cos\varphi} \quad (11)$$

The beam tilt irregular spiral shape presents a problem: the slots will be closer together on the left side while on the right side, they will be sparser. First, the spiral is divided into 8 parts. The angle value of the axes intersection with the spiral is then retrieved and we characterize each arch by 2 values: the angle at the start β_I, and at the end β_F. The

number of pairs m is chosen for each arch. The difference between the arch angle of start and finish, represented by β_D, is divided by in equal parts, m – 1, to ensure an even and equidistant distribution. The following equations express the method and Figure 4 shows an illustration:

$$\beta_{\mathrm{D}} = \beta_{\mathrm{F}} - \beta_I \tag{12}$$

$$\mathrm{C} = \frac{\beta_{\mathrm{d}}}{\mathrm{m} - 1} \tag{13}$$

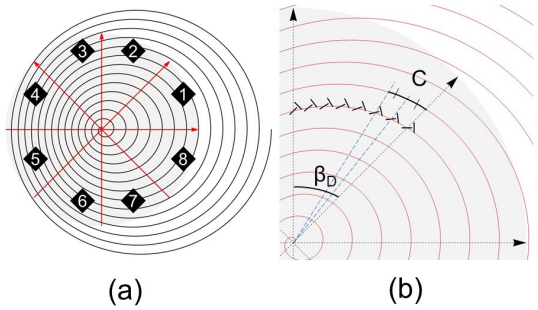

Figure 4: Method to fulfil slot pair distribution: Sectionalization of the RLSA into eight parts (a) and the method for positioning the slots in one single arch (b)

3. Simulations Results

3.1. PPW design and optimization

3.1.1 Plates

The variables considered are plate radius, distance between plates and cables' core height inside the PPW and are referred as r_p, H and h_core. Both bottom and upper plates, are given a 0.15mm thickness and the coaxial cable for the excitation has 4.4mm of diameter. The materials used in the cable are copper for the core and PTFE (Teflon) for the dielectric surrounding the core. For the plates a PEC (Perfect electrical conductor) material is defined. The objective is to achieve an antenna with 150mm diameter, r_p = 75mm, as a result, coaxial cable and the PPW are tunned accordingly. From this section important information on the parameter is obtained: the bigger the distance between plates gets the less energy reflects back to the feed; the higher the cable inside the PPW, the poorer the reflection coefficient $S_{1,1}$ becomes.

3.1.2 Absorver rim

To decrease internal reflections, placing an absorber rim at the perimeter of the antenna is regarded as an option. ECCOSORB AN-77 is chosen as the material for the simulations. Figure **??** presents que AN-77 material at the edge of the structure. λ_0 is found to be the ideal thickness to counteract the effects of internal relfections.

3.1.3 Dielectric Substrates

The option of filling the inside of the PPW with a dielectric substrate is studied. Duroid 5880 and FR-4 are the materials tested. Duroid 5880 has a relative electric permittivity of $\epsilon_r = 2.2$ and FR-4 $\epsilon_r = 4.4$. Different values of ϵ_r, translates to different wavelengths, equation (2). Table 1 represents the different wavelengths.

	Air	Duroid 5880	FR-4
ϵ_r	1	2.2	4.2
λ_g[mm]	10	6.74	4.87

Table 1: Guided Wavelengths for different dielectric materials: air, Duroid 5880 and FR-4.

For H, air and FR-4 simulations are kept at H=1.5mm while for Duroid 5880 a slighty higher value is considered, H=1.575mm, since it is the thickness available in the laboratory. Figure 5 shows the comparison.

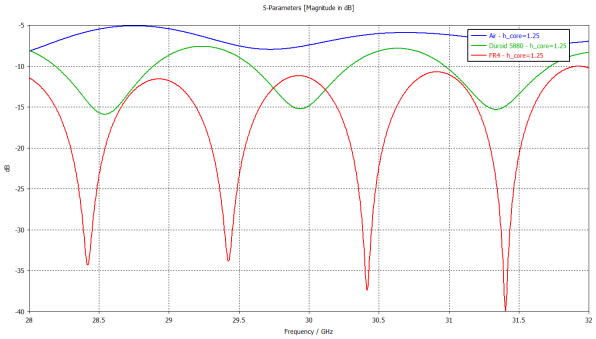

Figure 5: S1,1 for a PPW with rp = 75mm and h_core = 1.25mm and different dielectric substrates: Air H = 1.5mm (blue), Duroid 5880 H = 1.575mm (green) and FR-4 H = 1.5mm (red)

The possibility of using any of these materials needs further analysis because there are other factors to take into consideration.

3.2. Aperture design

3.2.1 Slot Dimensions

To study slot length a structure modelled after a quarter of a PPW and of a single slot pair place upon the top plate is designed. ECCOSORB AN-77, is placed at the edge to minimize reflected wave disturbances to the field that may occur. Additionally, to feed the structure, a discrete wave port is placed at the origin of the structure to carry out excitation and, the open-ended sides boundaries magnetic fields in planes YZ and XZ are null. Figure 6 shows the model. The pair radial distance is varied and the length of the slots is also varied [3.0;7.5] mm. Slot width is kept constant, W = 0.5mm.

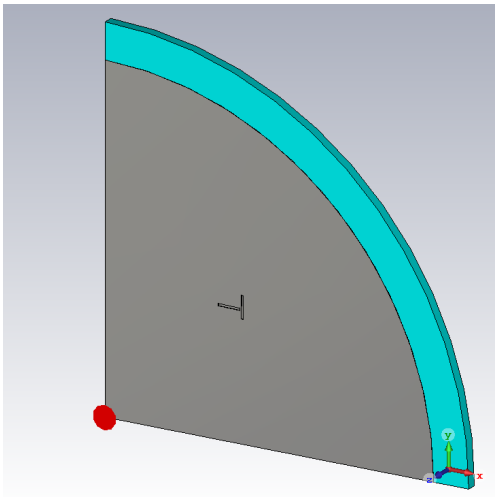

Figure 6: Slot dimension study model in CST STUDIO Suite: one quarter of a PPW with a single slot pair on top

Slot with a length of 4.0mm, 4.5mm, 5.0mm and 5.5mm seem to perform better. As the length gets closer to half guided wavelength $\frac{\lambda_0}{2}$, the fields are greater, meaning the length becomes more resonant with the fields.

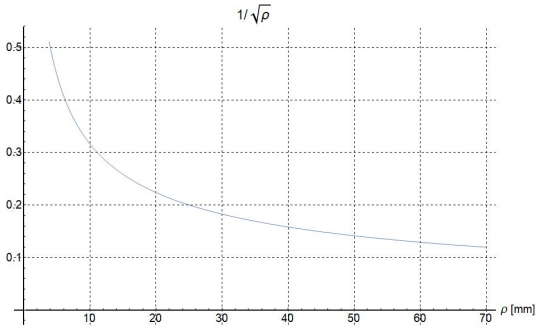

Figure 7: Plotted function of $\frac{1}{\sqrt{\rho}}$

Field behaviour at all slot lengths at each radial distance point are inversely proportional to the radial distance square root as it is expressed in equation (5) and ilustrated in Figure 7.

3.2.2 Slot Distribution

The substrate is chosen based on performance. All three materials are tested for a reduced number of slots and for each one, $L = \frac{\lambda_g}{2}$ and $W = \frac{\lambda_g}{20}$. FR-4 and Duroid 5880 substrates radiation efficiency and S1,1 are smaller in contrast with air, with the latter being the lower of all three cases. FR-4 has the lowest X-Pol levels and the increase in directivity is small. Duroid 5880 presents the highest directivity and best X-Pol levels of all the three. Air presents the best values for radiation efficiency and S1,1. Based on the analysis, FR-4 is discarded from further examination. Duroid 5880 and air continue to be considered. Two fully completed RLSA antennas are tested for air and Duroid 5880. Figure 8 showns thr models.

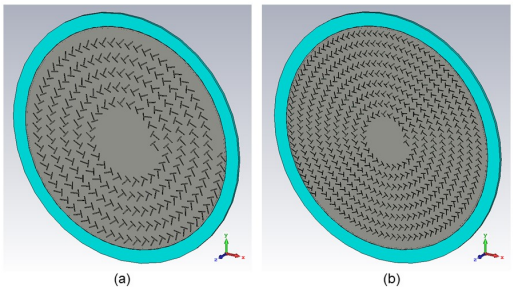

Figure 8: Complete RLSA model for air (a) and Duroid 5880 (b) in CST STUDIO Suite

Simulations result in a 29.35 dB directivity for Duroid 5880 and a 22.25dB directivity for air @30GHz. $S_{1,1}$ levels are better for Duroid 5880, -12.54dB, but X-Pol levels and radiation efficiency, -13.11dB and -2.72dB, respectively. For air, $S_{1,1}$=-4.85dB, X-Pol=-23.0dB and Rad.Efficiency=-0.11dB. Duroid is chosen for its directivity and $S_{1,1}$ levels. To achieve better performance the slot dimensions, L and W, are modified. It is understood that a change in slot length will produce a shift in the operating frequency. Best results are found at 28.6GHz for slot dimensions of L = 3.74mm and W = 0.4mm. Figure 9 and Figure 10 present the results for the new slot dimensions.

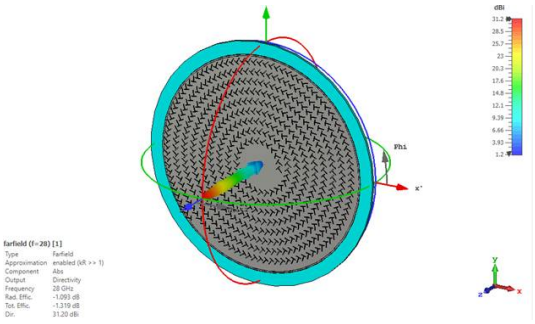

Figure 9: Farfield 3D Radiation Pattern @ 28.6GHz for L = 3.74mm and W = 0.4mm.

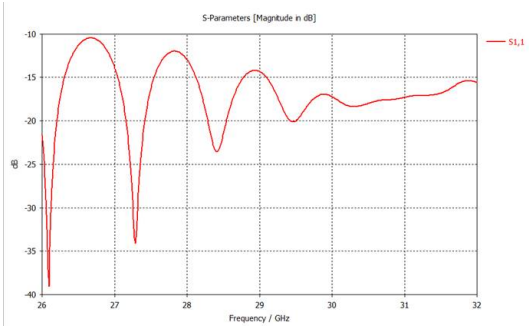

Figure 10: S1,1 levels for a completed RLSA @ 28.6GHz for L = 3.74mm and W = 0.4mm

3.3. Beam tilt Aperture Design

For the beam tilt design slot pairs are placed according to a spiral produced by equation (11) for a $\alpha_0 = 25.4^o$. Multiple lengths are tested and the best value is 3.6mm @28.6GHz. Directivity is 28.85dB

ans $S_{1,1}$ levels are good, -19.0dB. The antenna has a better X-Pol level of -17.4dB and a radiation efficiency of -1.154dB. Figure 11 and Figure 12 present the results for the design.

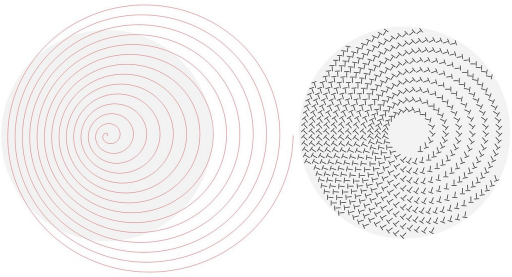

Figure 11: Spiral and subsquent slot array for a α_0 = 25.4º beam tilt RLSA antenna

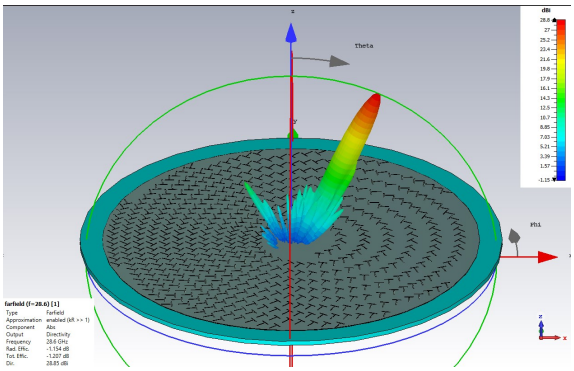

Figure 12: Farfield 3D Radiation Pattern for Beam Tilted RLSA, α_0 = 25.4º, L=3.6mm

3.4. New Feed design

The first step of the design is to define the parameters intervals. The cavity radius, r_{cavity}, is tested using $\frac{\lambda_0}{4}$ increments until it reaches the point where the first pair of slots is found. The height, h_{cavity}, follows the condition (2.5) and is tested in the interval [1;5]mm with 0.5mm steps. The height of the cable, h_{cable}, is tested according to h_{cavity}. It goes from the lowest setting to the maximum height possible. The entry hole for the cable, din, depends on the cable being used. For the feed, coaxial cable EZ-86 is chosen. Figure 13 shows the feeding structure.

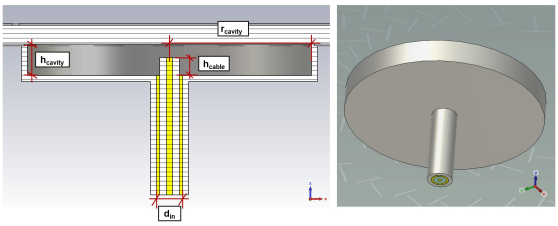

Figure 13: New feed for RLSA antennas

No solution for the feed measures stand out. $S_{1,1}$ levels for $r_{cavity} = 12.5mm$ $h_{cavity} = 2.5mm$ $h_{cable} = 1.5mm$ have dips in frequencies from previous iterations of the antenna. For that reason, these measures are chosen. Figure 14 shows $S_{1,1}$ levels for the current feed dimensions.

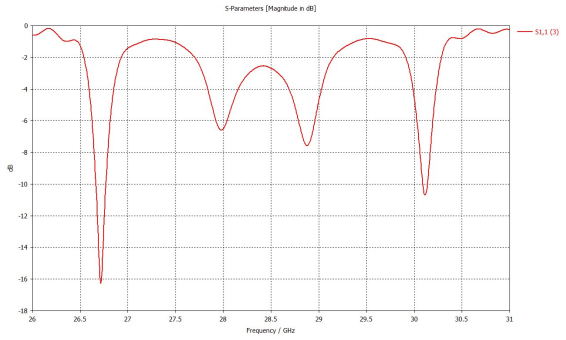

Figure 14: $S_{1,1}$ levels for $r_{cavity} = 12.5mm$ $h_{cavity} = 2.5mm$ $h_{cable} = 1.5mm$

All the tests are performed in a structure with no slots thus, further adjustments are needed when attaching the feed and RLSA antenna.

3.5. Final CP-RLSA models

Modifications occur when attaching the new feed and the RLSA. The absorbent is no longer considered. Absorbent thickness proposed is not viable because it is too thin. A re-tunning of the new feeding cavity for the previously established RLSA is made and a the optimal vaules for the cavity achieved @29.1GHz. Table 2 summarizes the results. RLSA antenna with α_0 has 1072 slots (536 pairs) and RLSA antenna with α_0 = 25.4º has 998 slots (499 pairs). Figure 15 represents the S1,1 for the final designed RLSA. The two RLSA antennas have final bandwidth of approximately 800MHz (frequency band bellow -10dB).

	$\alpha_0 = 0º$	$\alpha_0 = 25.4º$
H [mm]	1.575	1.575
L [mm]	3.74	3.6
W [mm]	0.4	0.4
r_{cavity}	12	12
h_{cavity}	2.5	2.5
h_{cable}	1.5	1.5
Realized Gain [dB]	29.33	26.45
S1,1 [dB]	-22.0	-13.2
X-POL [dB]	-7.99	-28.0
SLL [dB]	-19.4	-11.1
Rad. Efficiency [dB]	-0.15	-0.12
Total Efficiency [dB]	-0.18	-0.33

Table 2: RLSA antenna parameter results @ 29.1 GHz

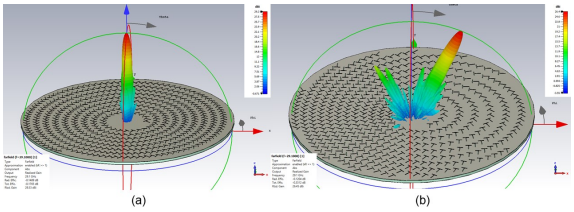

Figure 15: Farfield Realized Gain 3D Radiation Pattern@29.1GHz: $\alpha_0 = 0^{\text{o}}$ (a) and $\alpha_0 = 25.4^{\text{o}}$ (b).

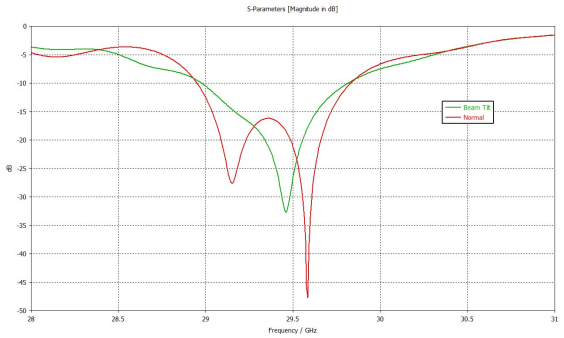

Figure 16: S1,1 for both final RLSA simulated models: $\alpha_0 = 0^{\text{o}}$ (red) and $\alpha_0 = 25.4^{\text{o}}$ (green)

3.6. Manufacture process

To validate both RLSA designs, two prototypes will be constructed. Some components are finished and others are in the final stages of fabrication.

3.6.1 Feed Cavity

The final model is made out of brass. There are slight variations, but the main parameters remain the same: $r_{cavity} = 12.5mm$ and $h_{cavity} = 2.5mm$. The walls increased in thickness to 1 mm to ensure a sturdy structure and a small ledge is added on top of the cavity walls to facilitate the junction between the cavity, and the bottom plate. An extra piece is added to the bottom of the structure. A bolting nut is used to secure the coaxial cable in place and allow more precise adjustments. 17 shows the final result.

Figure 17: Feed cavity final constructed model

3.6.2 Printed Circuit

The manufacture of the top and bottom plate of the antennas is accomplished through a printed process. From the CAD models developed in CST STUDIO Suite, 4 masks are generated: for a normal beam, for a beam tilted beam and ground plate masks. 18 shows the three masks used to print on both sides of a ROGER 5880 substrate with 1.57 5mm.

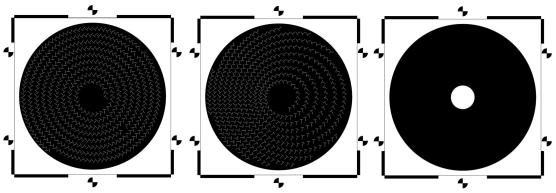

Figure 18: Masks used for the production of the printed circuit

3.6.3 Antenna support

To hold the antenna in place a support structure is devised. 19 represents the CAD model conceived. The support is adapted for a previously constructed platform, represented in the 19 in blue. It is comprised of a central ring with 8 holes to fit screws and 3 arms separated by 120^{o}. At the end of each arm there is a claw which holds the RLSA antenna. Each claw is screwed to the respective arm.

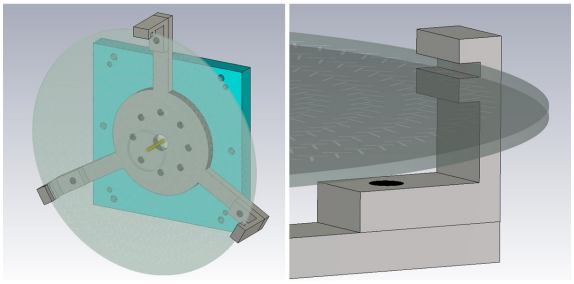

Figure 19: CAD antenna support model

4. Conclusions

The two antennas in this work are developed for user satellite access in the k_a band. The first RLSA antenna radiates parallel to the normal direction, $\alpha_0 = 0^{\text{o}}$, and the second RLSA antenna radiates at an angle of $\alpha_0 = 25.4^{\text{o}}$ relative to the normal direction. They both have a 150mm diameter and are fed by a new designed cavity and a coaxial cable placed under the structure. The first one averages a 29.3dB gain and the second a 26.4dB. They both present a good SLL when considering the main lobe direction. By examining S1,1, their bandwidth is roughly 800MHz. X-Pol levels obtained are not ideal for the first RLSA and good for the second RLSA. Improvements on the X-Pol, gain and efficiency of the antennas are left for future study.

Acknowledgements

I would like to thank Instituto de Telecomunicacões, UIDB/50008/2020, and project ADAM3D: PTDC/EEITEL/30323/2017, for financing all the needed material used in this thesis, and for the usage of IT laboratories, software and hardware equipment.

References

[1] C. A. Balanis. *Antenna Theory - Analysis and Design*. 4th Ed. John Wiley Sons, 2016.

[2] F. Goebels and K. Kelly. Arbitrarily polarized planar antennas. 1963.

[3] A. M. M. Albani and A. Freni. Automatic design of cp-rlsa antennas. *IEEE Trans. Antennas Propag., vol. 60, no. 12, pp. 5538–5547*, 2012.

[4] J. T. M. Ando, M. Takahashi and N. Goto. A slot design for uniform aperture field distribution in single-layered radial line slot antennas. *IEEE Antennas and Propagation Society, AP-S International Symposium (Digest) vol. 2, pp. 930–933*, 1991.

[5] K. S. M. Ando and N. Goto. Characteristics of a radial line slot antenna for 12 ghz band satellite tv reception. *IEEE Trans. Antennas Propag., vol. 34, no. 10, pp. 1269–1272*, 1986.

[6] K. S. M. Ando and N. Goto. A radial line slot antenna for 12 ghz band satellite tv reception. *IEEE Trans. Antennas Propag. vol. 34, no. 10, pp. 1269–1272*, 1986.

[7] M. N. J. T. M. Ando, M. Takahashi and N. Goto. Single-layered radial line slot antenna for dbs reception. *Conference Proceedings - European Microwave Conference, vol. 2, no. 20*, 1990.

[8] D. V. V. M. J. Lopez-Morales, F. R. Varela and M. S. Castaner. Efficient design of radial line slot antennas using currents synthesis and optimization. *IEEE Antennas Wirel. Propag. Lett., vol. 19, no. 3, pp. 487–491*, 2020.

[9] M. Y. M. Takahashi and M. Abe. Basic design of beam tilting radial line slot antennas. *IEEE Antennas Propag. Soc. AP-S Int. Symp., vol. 3, pp. 1384–1387*, 1995.

[10] M. S.-C. M. Vera-Isasa and M. Sierra-Pérez. Slot antenna with a tilted beam for satellite reception. *Microw. Opt. Technol. Lett., vol. 36, no. 5, pp. 392–394*, 2003.

[11] M. S.-C. M. Vera-Isasa and M. Sierra-Pérez. Design of mm-wave rlsas with lossy waveguides by slot coupling control techniques. *IEICE Transactions on Communications, E98B, n. 9, pp. 1865-1872*, 2015.